Neurobiology of Aging 80 (2019) 91–98

Contents lists available at ScienceDirect

Neurobiology of Aging

journal homepage: www.elsevier.com/locate/neuaging

T2*-weighted MRI values correlate with motor and cognitive dysfunction in Parkinson's disease

Nicola Tambasco [a,*], Federico Paolini Paoletti [a], Andrea Chiappiniello [b], Viviana Lisetti [c], Pasquale Nigro [a], Paolo Eusebi [a], Pietro Chiarini [d], Michele Romoli [a], Elona Brahimi [a], Simone Simoni [a], Marta Filidei [a], Piero Floridi [d], Roberto Tarducci [e], Lucilla Parnetti [a,c], Paolo Calabresi [a,c,f]

[a] Neurology Department, University of Perugia, Santa Maria della Misericordia Hospital, Perugia, Italy
[b] Physics and Geology Department, University of Perugia, Perugia, Italy
[c] Section of Neurology Department, Center for Memory Disturbances, Laboratory of Clinical Neurochemistry, University of Perugia, Santa Maria della Misericordia Hospital, Perugia, Italy
[d] Neuroradiology Unit, Radiodiagnostic Department, Santa Maria della Misericordia Hospital, Perugia, Italy
[e] Medical Physics Unit, Santa Maria della Misericordia Hospital, Perugia, Italy
[f] Experimental Neurophysiology Laboratory, I.R.C.C.S. Fondazione Santa Lucia, Roma, Italy

ARTICLE INFO

Article history:
Received 15 August 2018
Received in revised form 4 April 2019
Accepted 5 April 2019
Available online 11 April 2019

Keywords:
Parkinson's disease
Cognitive impairment
Brain iron
Magnetic resonance imaging
Susceptibility-weighted imaging

ABSTRACT

Brain iron load is one of the main neuropathologic hallmarks of Parkinson's disease (PD). Previous studies indicated that iron in the substantia nigra (SN) is related to disease duration and motor impairment. We explore, through a cross-sectional study, the association between brain iron distribution, evaluated by T2*-weighted magnetic resonance imaging (T2*), and clinical features in a cohort of patients with PD. Thirty-two patients with PD, compared with 10 control subjects, were evaluated for motor and cognitive features (attention and working memory, executive functions, language, memory, and visuospatial function). They underwent a magnetic resonance imaging protocol including T2* analysis of specific brain regions of interest to measure iron load compared with healthy control subjects. We found that iron content of the SN correlated positively with both disease duration and *Unified Parkinson's Disease Rating Scale III off* score. *Montreal Cognitive Assessment*, *Spatial Span*, and *Graded Naming Test* scores were inversely associated with iron load of the SN, whereas Wechsler Adult Intelligence Scale-IV *Similarities* score showed an inverse relationship with iron content in all the regions of interest examined. Our findings suggest a relationship between topographic brain iron distribution and cognitive domain impairment.

1. Introduction

Parkinson's disease (PD) is a progressive neurodegenerative disease characterized by movement disorders and nonmotor symptoms of which cognitive impairment is the most frequent (Aarsland et al., 2017). Brain iron load is for PD, a neuropathologic hallmark that can be evaluated by magnetic resonance imaging (MRI). Physiologically, iron homeostasis is needed to sustain normal brain functions (Anderson et al., 2009; Bartzokis et al., 2004; Simpson et al., 2015). On the other hand, dysregulation of iron metabolism is known to be implicated in PD mechanisms linked to neurodegeneration. Several findings have provided a potential involvement of iron accumulation in the nigral cell death in PD. However, it seems that excessive brain iron deposition is not a simple consequence of neuronal cell death but rather a causative factor in processes leading to neurodegenerative changes (Apostolakis and Kypraiou, 2017). The alterations of iron metabolism can occur at different levels and they are linked to a multifactorial pathogenesis, related to genetic and nongenetic factors (Ke and Qian, 2003). It is well accepted that one of the main mechanisms by which iron causes neurotoxicity in PD is the increased generation of reactive oxygen species that in turn damage cellular components and facilitate protein aggregation, including α-synuclein aggregation (Zecca et al., 2004). However, it has been controversial whether the iron accumulation is a primary causative event or merely a secondary change related to the dopaminergic neuronal degeneration (Mochizuki and Yasuda, 2012). Consequently, iron-mediated neurotoxicity is one possible mechanism.

* Corresponding author at: Neurology Department, University of Perugia, Santa Maria della Misericordia Hospital, S. Andrea delle Fratte, 06156 Perugia, Italy. Tel.: +39 075 5783830; fax: +39 075 5784229.
E-mail address: n.tambasco@libero.it (N. Tambasco).

0197-4580/$ – see front matter © 2019 Published by Elsevier Inc.
https://doi.org/10.1016/j.neurobiolaging.2019.04.005

Iron is characterized by an inhomogeneous distribution in the central nervous system and it is predominant in brain regions related to motor functions, such as the corpus striatum and the substantia nigra (SN), where its levels increase with aging (Valdés-Hernández et al., 2016). The pioneering postmortem studies of Hallgren and Sourander (1958) show how in the globus pallidus (GP), SN, red nucleus (RN), and dentate nucleus (DN) iron increases rapidly from birth until the end of the second decade, plateaus for several years, and then shows another milder increase after age 60 years. Moreover, some findings suggest that iron deposits of the basal ganglia are closely related to worst cognitive performance and seem to be a biomarker of age-related cognitive decline (Penke et al., 2012).

The advent of specific MRI techniques made it possible to evaluate brain iron deposits in vivo. So far, R2-weighted, R2*-weighted, and neuromelanin imaging have been used to assess brain iron pattern. However, relaxation rates R2 and R2* are influenced not only by iron deposition but also by tissue water changes that interfere on relationship between iron and R2, R2* parameters (Ordidge et al., 1994). This is one of the main reasons leading to investigate newer MRI protocols and parameters to quantify brain iron.

So far, studies exploring, by means of MRI, the relationship existing between brain iron load and clinical features of patients with PD gave uncertain results (Brooks and Tambasco, 2016). Thus, our purpose was to investigate the role of T2*-weighted imaging, that is, sensitive to susceptibility changes. The possible correlations between motor disturbances, cognitive impairment, and brain iron levels were evaluated in a group of patients with PD.

2. Materials and methods

2.1. Participants

Thirty-two patients with PD and 10 control subjects were consecutively included in the present study for more than a period of 4 years. Subjects were consecutively recruited among outpatients from Movement Disorders Center of the Neurology Department of University Hospital in Perugia. Clinical diagnosis of PD was established according to the Movement Disorders Society (MDS) clinical diagnostic criteria for Parkinson's disease (Postuma et al., 2015). The main demographic and clinical characteristics of the subjects were assessed by 2 experienced neurologists (P.N. and F.P.P.). All patients were on dopaminergic therapy. Therapy was not modified during the study. Similarly, control subjects were recruited among supporting persons (not familiar) of the outpatients negative for neurologic diseases. Both patients and control subjects gave their written informed consent to the study. The study was approved by the local Ethics Committee (CEAS Umbria).

2.2. Clinical examination

2.2.1. Motor evaluation

Clinical motor impairment was rated according to the examination of the Unified Parkinson's Disease Rating Scale (*UPDRS*)-*III* (Goetz et al., 2008), before (*off*) and after (*on*) levodopa administration. Disease-related disability was assessed by means of Hoehn and Yahr scale (Goetz et al., 2004). Patients were also examined for the possible presence of motor fluctuations, dyskinesia, and other medication-related complications. Functional abilities were assessed with the activities of daily living (ADL) (Katz et al., 1963) and the instrumental ADL scales (Lawton and Brody, 1969).

2.2.2. Neuropsychological evaluation

In patients with PD, cognitive functioning was assessed according to the MDS Task Force recommendations (Litvan et al., 2012), within 1 week of the MRI session by a 2-level operational schema using a series of neuropsychological tests assessing general and specific cognitive functions. The first level (level I) was represented by global cognitive functioning, which was measured using the *Montreal Cognitive Assessment* (MoCA) (Gill et al., 2008) and *Mini-Mental State Examination* (MMSE) (Folstein et al., 1975). The second level (level II) was characterized by cognitive tests that were administered in a fixed order by an expert neuropsychologist and categorized into 5 domains: (1) Attention and working memory: *digits forward/backward* (Monaco et al., 2013), *Spatial Span* and *Simple Reaction Time* (CANTAB Cambridge Cognition, 2006a). (2) Executive functions: *Phonemic* (Carlesimo et al., 1995, 1996) and *Semantic Fluency Test* (Novelli et al., 1986) and *Stockings of Cambridge* (CANTAB Cambridge Cognition, 2006a). (3) Language: *WAIS-IV Similarities* (Wechsler, 2008) and *Graded Naming Test* (CANTAB Cambridge Cognition, 2006a). (4) Memory: *Wechsler Memory Scale-IV Logical Memory Subtest* (Wechsler, 1987) and *Pattern Recognition Memory* (CANTAB Cambridge Cognition, 2006a). (5) Visuospatial function: *Clock Drawing Test* (Caffarra et al., 2011) and *Pentagons Copy* (Cormack et al., 2004).

Control subjects underwent a neuropsychological assessment including MMSE, MoCA, and Milan Overall Dementia Assessment (Brazzelli, 1994), to evaluate all cognitive domains. All of them scored within normal range.

2.3. Image acquisition and processing

2.3.1. MRI protocol

Patients and control subjects underwent MRI acquisition on a 3.0 T Philips Achieva system, using an 8-channel head coil. The MRI protocol included an anatomic fluid-attenuated inversion recovery sequence (axial acquisition, field of view = 230 × 230 mm^2, pixel size = 0.45 × 0.45 mm^2, slice thickness = 4 mm, number of slices = 29 with a slice gap of 1 mm, echo time (TE) = 125 ms, repetition time (TR) = 11,000 ms, flip angle = 90°, no fat suppression, full k-space, no averages) and a 3-dimensional multishot fast field echo-planar imaging sequence sensitive to T2* changes (FOV = 220 × 220 mm^2, pixel size = 0.45 × 0.45 mm^2, slice thickness = 1 mm, number of slices = 200 without slice gap, TE = 21 ms, TR = 15 ms, flip angle = 10°, no fat suppression, full k-space, no averages). In particular, the magnitude signal-intensity response in the T2*-weighted sequence (radio-frequency-spoiled short-TR gradient echo sequence) is given by

$$s_m(\alpha) = \rho \cdot \sin(\alpha) \cdot e^{-\frac{TE}{T2^*}} \cdot \frac{1 - e^{-\frac{TR}{T1}}}{1 - \cos(\alpha) \cdot e^{-\frac{TR}{T1}}}$$

where ρ is the spin density of the tissue, TE is the echo-time, TR is the repetition-time of each data acquisition, α is the (magnetization) flip angle, T1 is longitudinal relaxation time of the tissue, and T2* is the transverse relaxation time considering the B_0 static magnetic field inhomogeneities (Haacke et al., 2009).

2.3.2. Image processing

Dicom data were converted to the neuroimaging informatics technology initiative format using the free *dcm2nii* software (http://www.mccauslandcenter.sc.edu/mricro/mricron/dcm2nii.html, output format SPM8—3D NIFTI) to properly process the images.

T2*-weighted images were considered for the quantitative analysis. A coregistration between FLAIR and T2*-weighted images was performed by Statistical Parametric Mapping-12. The additional contrast provided by FLAIR allowed a double check in the positioning of the regions of interest (ROIs) on T2*-weighted

images. FLAIR images were also used to exclude secondary lesions by visual inspection.

The placement of ROIs was carried out by a trained investigator, who was blind to the clinical status of each subject (patient with PD or control subject). ROIs were chosen on the basis of others and our previous work (Tambasco et al., 2011; Ward et al., 2014; Zhang et al., 2010). In particular, for each hemisphere, 7 ROIs were considered: putamen (PU), GP, caudate nucleus (CN), RN, SN, DN, and frontal white matter (FWM) (Fig. 1). ROIs analysis was done using ImageJ (Rasband, W.S., ImageJ, U. S. National Institutes of Health, Bethesda, MD, USA, http://imagej.nih.gov/ij/, 1997–2016). Moreover, we included a deep white matter ROI in the frontal lobe and in the same axial sequence of the basal ganglia as a control ROI of the white matter. Furthermore, to limit bias from signal heterogeneity, ROIs were chosen in the most homogenous region (Haacke et al., 2007). For each ROI, mean intensity value and intensity standard deviation were evaluated. Lower values correspond to higher iron content.

First, the ROIs were manually traced on the T2*-weighted images and directly transferred to the coregistered FLAIR. ROIs were drawn and magnified 4 times before tracing to obtain means and standard deviations of the image intensity in the ROIs. To avoid partial volume effects, ROI boundaries were traced, as far as possible, from the gray-white matter junction and not very close to the edge of the selected targets. The ROIs of the subcortical nuclei were drawn according to the anatomic structures, including RN, SN, CN, GP, PU whereas in the FWM the ROIs were circular. Finally, the obtained measurements converted from the intensity measurements were considered to be the putative iron concentrations in the ROIs.

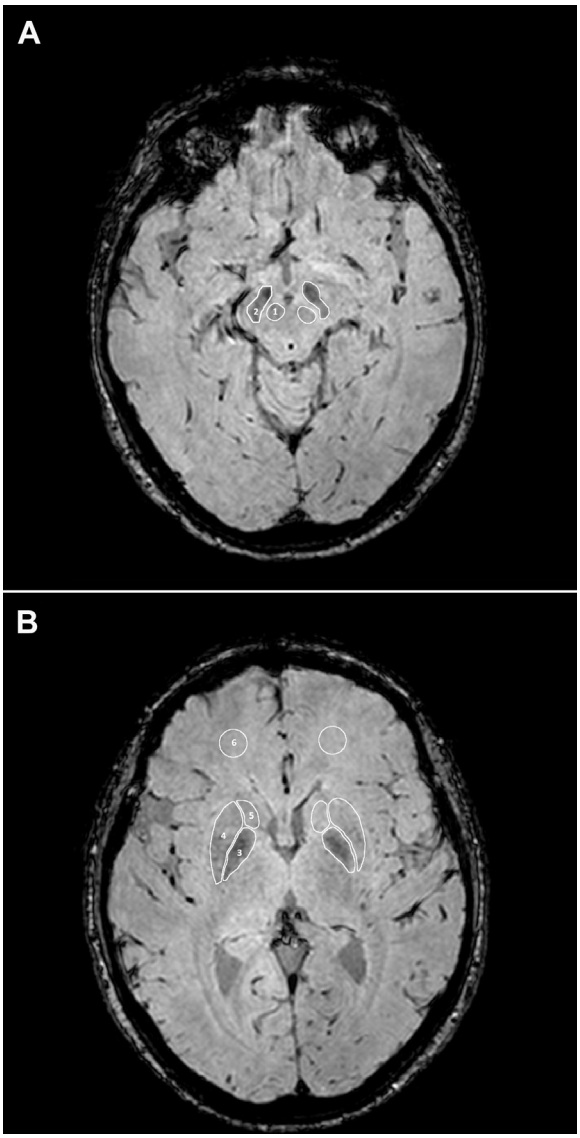

Fig. 1. Region of interest localization. The axial T2*-weighted MRI images show the region of interest in a patient with PD [1. red nucleus, 2. substantia nigra (A), 3. putamen, 4. globus pallidus, 5. head of the caudate nucleus, and 6. frontal white matter (B)]. MRI, magnetic resonance imaging.

2.4. Statistical analysis

Statistical analyses were performed using R software version 3.5 (R Development Core Team). Continuous variables were described by means and standard deviations, whereas categorical ones were reported as count and percentages. The χ^2 test was used for verifying the associations between categorical variables, and Student's *t* test was used for investigating the difference in continuous variables between groups. Pearson coefficients were calculated for measuring correlations between continuous variables. Partial correlation coefficients were calculated for taking into account age and gender as potential confounders. Holm-Bonferroni procedure was used for controlling the familywise error rate. We performed intraclass correlation coefficient as a measure of interobserver and intraobserver reliability. Distribution of variables was checked for normality with Shapiro-Wilk test. When appropriate, nonparametric analyses were carried out. ROI measures and age entered in a partial least squares generalized linear model (Ding and Gentleman, 2005) that was fitted to discriminate PD and control subjects, because of robustness of approach in circumstances where there is multicollinearity in the predictors. We carried out 10-times 10-fold cross-validation with caret R package (Kuhn, 2008). Resampling results were evaluated in terms of accuracy across tuning parameters, including number of components to be extracted. Significance level of 5% was assumed for all the analyses.

3. Results

3.1. Demographic and clinical characteristics

The analysis was carried out on 32 patients and 10 control subjects. Demographic and clinical features of PD patients are shown in Table 1. Age and gender were comparable across patients and control subjects.

3.2. MRI results

To verify the quantification of iron content, we calculated mean iron deposition for each area of the patient group of Martin et al.

Table 1
Average ± demographics and clinical features SD or number (%)

	PD	Control subjects	*p* value
Numbers	32	10	—
Sex (Male)	20 (62%)	6 (60%)	1.000
Age (y)	58.2 ± 9.8	59.0 ± 8.7	0.836
Disease duration (y)	3.9 ± 3.4	—	—
UPDRS-off	23.9 ± 11.0	—	—
UPDRS-on	15.3 ± 7.5	—	—
H&Y	1.9 ± 0.8	—	—
MoCA	23.0 ± 2.7	—	—
ADL	5.8 ± 0.5	—	—
IADL	7.5 ± 1.7	—	—

Key: ADL, activities of daily living; H&Y, Hoehn and Yahr scale; IADL, instrumental activities of daily living; MoCA, Montreal Cognitive Assessment; PD, Parkinson's disease; SD, standard deviation; UPDRS, Unified Parkinson's Disease Rating Scale.

(2008) correlating with the values of our group. The correlation value was −0.81 ($p = 0.002$). The correlation is negative because R2 and T2* are one of the reciprocals of the other (R2* = 1/T2*).

One patient dropped out for MRI evaluation because of motion artifacts, so MRI analysis was carried out on 31 patients. Both patients and control subjects did not show significant differences in T2*-weighted values between the 2 hemispheres within each ROI, with left-right correlations ranging from 0.72 (SN) to 0.90 (RN). Therefore, left and right values were averaged for each ROI. Both patients and control subjects showed lower T2*-weighted values in the GP, whereas FWM was the region with higher values. In patients with PD lower T2*-weighted values were detected in all the ROIs compared with control subjects, indicating higher iron deposition, although the difference between the 2 groups was not statistically significant (Fig. 2). However, when entered in the partial least squares generalized linear model, ROIs discriminated PD and control subjects with a fair accuracy (79%) with PU, CN, and FWM being mostly related to the single-dimensional component extracted.

Spearman's correlation between T2* values and age, that is an independent factors of brain iron accumulation, showed a direct relationship with T2* values indicating an effect of age on brain iron deposition. All the ROIs showed negative correlation between T2* and age, with Pearson correlation coefficients ranging from −0.05 in FWM to −0.40 in PU-. In all the patients only in PU we found as significant correlation ($r = -0.40$, $p = 0.010$) whereas in PD we found significant associations in PU ($r = -0.47$, $p = 0.010$), globus pallidus ($r = -0.46$, $p = 0.010$), and dentate nucleus ($r = -0.37$, $p = 0.040$). Hence, we considered age as a potential confounder for all the ROIs.

In patients with PD, a negative correlation was observed between duration disease and T2* values of the SN as a marker of degeneration with increased iron load ($r = -0.48$, $p = 0.009$).

3.3. T2*-weighted image values and motor function

In patients with PD, the UPDRS-III off score had a significant negative correlation with T2* values of the SN ($r = -0.48$, $p = 0.014$) and GP ($r = -0.45$, $p = 0.029$), whereas the UPDRS-III on score had a significant negative correlation only with T2* values of the GP ($r = -0.42$, $p = 0.048$). A significant positive relationship was found between ADL and instrumental ADL scales and T2* values of the SN ($r = 0.49$, $p = 0.028$) (Fig. 3). No significant correlations were found between T2* values and other explored clinical features such as motor fluctuations and dyskinesia. Taking into account age and gender as potential confounder, the T2* values of the GP had a significant negative correlation with UPDRS-III off score ($r = -0.40$, $p = 0.040$), as well as with the UPDRS-III on score ($r = -0.43$, $p = 0.027$). A significant negative relationship was also found between T2* values of the SN and UPDRS-III off score ($r = -0.48$, $p = 0.014$).

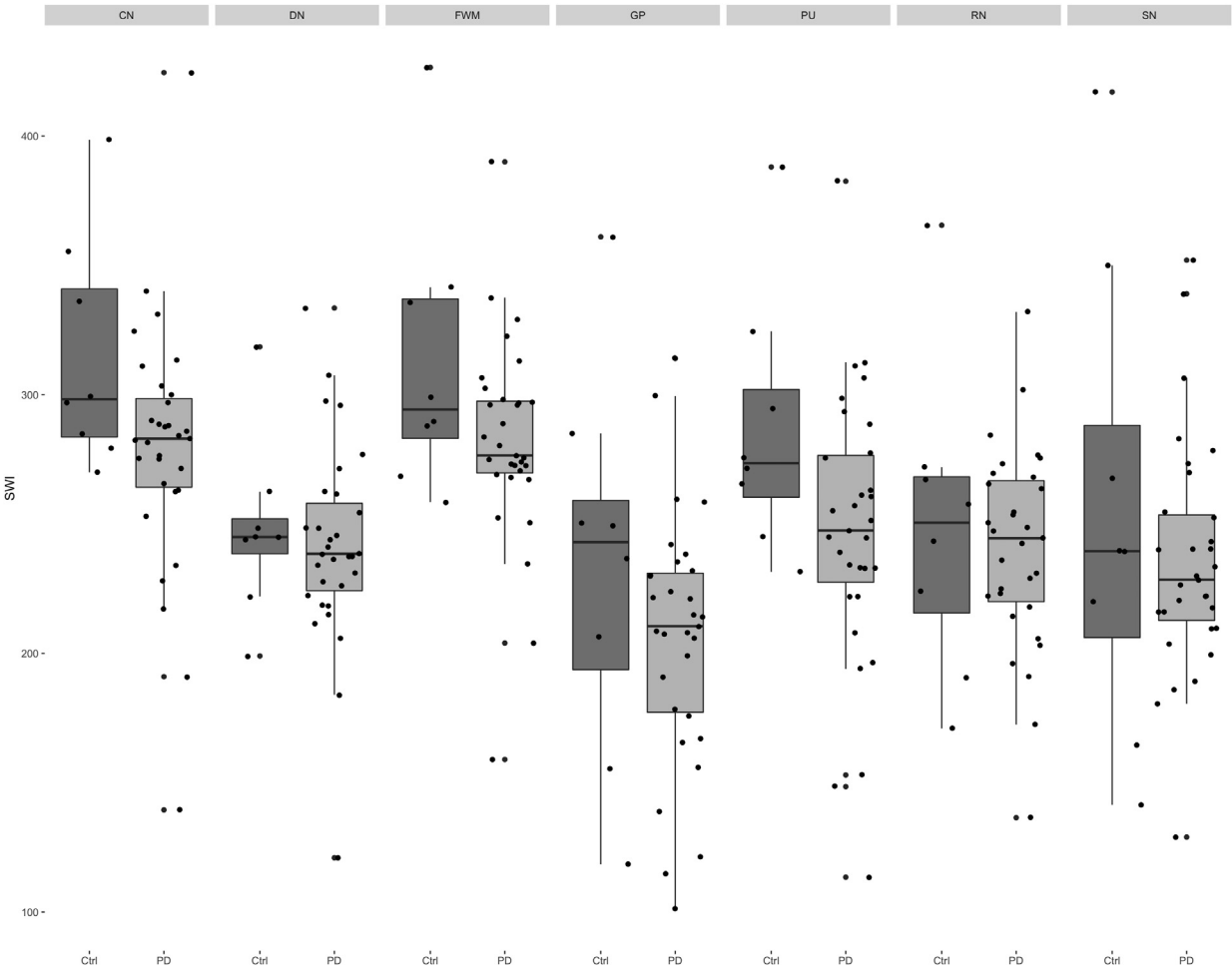

Fig. 2. T2* values detected in all the regions of interest (ROIs) between patients and control subjects. T2* values are lower in patients with Parkinson's disease compared with healthy subjects indicating that iron content is higher in patients compared with control subjects in all the ROIs we analyzed.

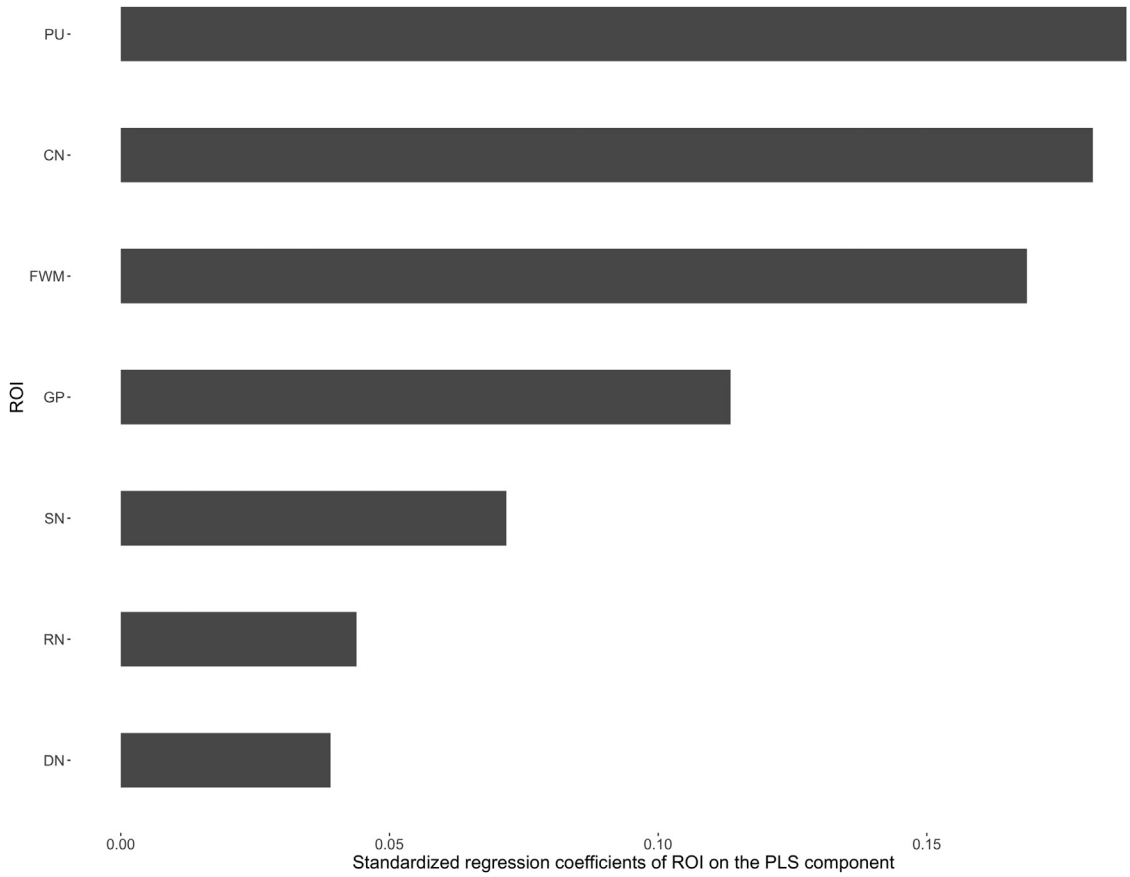

Fig. 3. Ranked standardized regression coefficients of partial least squares generalized linear model. Abbreviations: CN, caudate nucleus; DN, dentate nucleus; FWM, frontal white matter; GP, globus pallidus; PLS, partial least squares; PU, putamen; RN, red nucleus; ROI, region of interest; SN, substantia nigra.

3.4. T2-weighted image values and neuropsychological profile*

Level I: this level includes, according to Litvan et al. (2012), an impairment on a scale of global cognitive abilities validated for use in PD, represented by MoCA or MMSE. A positive correlation between MoCA score and T2* values of the SN ($r = 0.41$; $p = 0.041$) and GP ($r = 0.36$; $p = 0.048$) was found, whereas MMSE score had a significant positive correlation only with T2* value of the GP

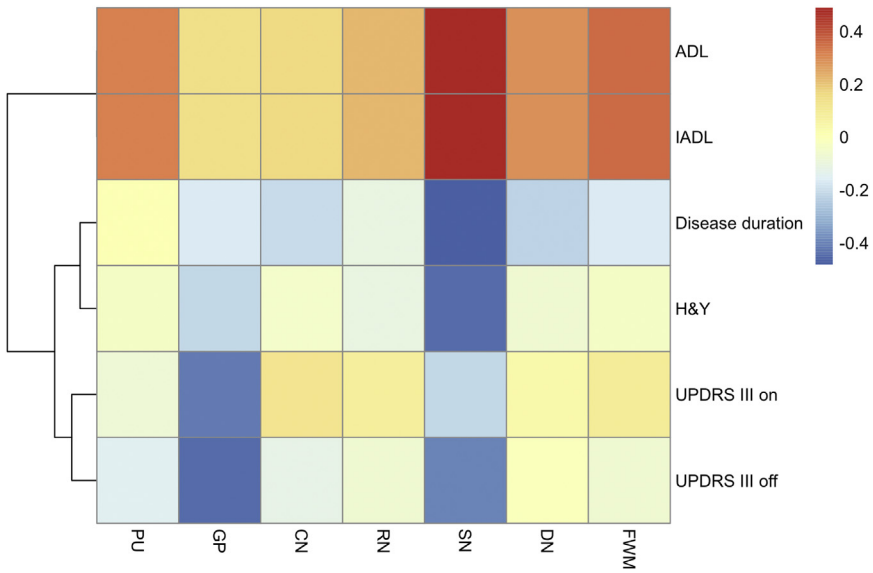

Fig. 4. Heatmap of correlations between motor features, ADL, IADL, disease duration, and T2* values. The heatmap colors range from negative correlation (blue) to positive correlation (red). Horizontal dendrogram added to the left show a meaningful clustering between motor features, ADL, IADL, and disease duration. Abbreviations: ADL, activities of daily living; H&Y, Hoehn and Yahr scale; IADL, instrumental activities of daily living; CN, caudate nucleus; DN, dentate nucleus; FWM, frontal white matter; GP, globus pallidus; PU, putamen; RN, red nucleus; SN, substantia nigra; UPDRS, Unified Parkinson's Disease Rating Scale. (For interpretation of the references to color in this figure legend, the reader is referred to the Web version of this article.)

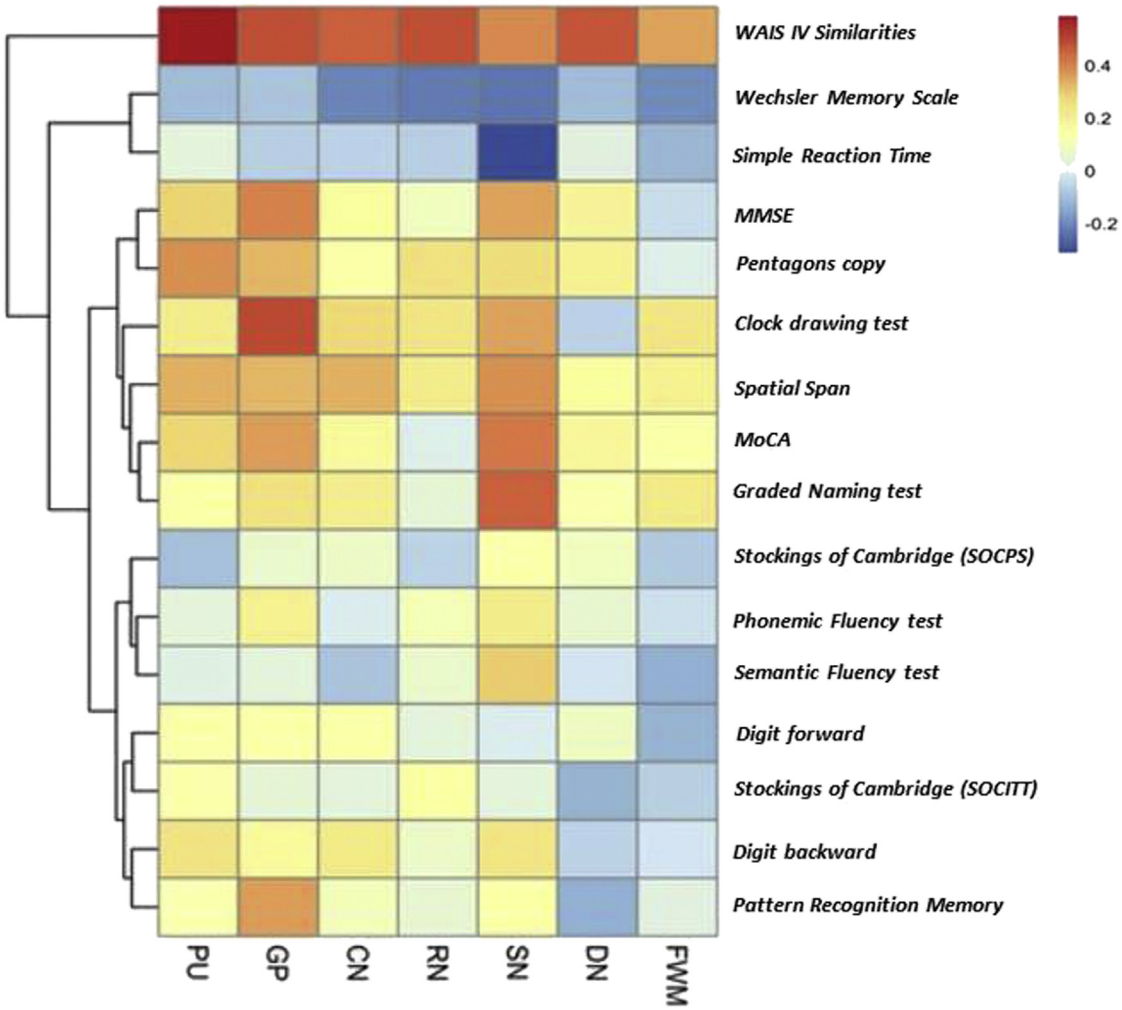

Fig. 5. Heatmap of correlations between neuropsychological tests scores and T2* values. The heatmap colors range from negative correlation (blue) to positive correlation (red). Horizontal dendrogram added to the left show a meaningful clustering between neuropsychological tests. Abbreviations: CN, caudate nucleus; DN, dentate nucleus; FWM, frontal white matter; GP, globus pallidus; MoCA, Montreal Cognitive Assessment; MMSE, Mini-Mental State Examination; PU, putamen; RN, red nucleus; SN, substantia nigra. (For interpretation of the references to color in this figure legend, the reader is referred to the Web version of this article.)

($r = 0.40$; $p = 0.049$). Taking into account the age and gender as potential confounders no significant relationships were found at level I neuropsychological scores.

Level II: as regards specific neuropsychological test, WAIS-R Similarities score showed to be a positive correlation with T2* values of all the examined ROIs, and in particular, with PU ($r = 0.59$; $p = 0.001$). Graded Naming Test score and Spatial Span score were positively correlated with T2* values of the SN (Graded Naming Test $r = 0.44$, $p = 0.032$; spatial span $r = 0.38$, $p = 0.049$) (Fig. 4). Taking into account the age and gender as potential confounder WAIS-R Similarities score showed to be positive correlated with T2* values of all the examined ROIs, and in particular with PU ($r = 0.54$; $p = 0.003$) (Fig. 5). Taking into account the age and gender as potential confounders Graded Naming Test score and Spatial Span score were positively correlated with T2* values of the SN (GNT $r = 0.38$, $p = 0.041$; SS $r = 0.48$, $p = 0.009$) (Fig. 5).

According to the 2 levels of neuropsychological evaluation, patients with PD were distributed as follows: 2 patients were demented, 3 patients were affected by mild cognitive impairment (MCI) involving amnestic domain, and 2 patients were affected by MCI multiple domain involving amnestic functions. The remaining patients showed neither MCI nor dementia. No significant differences were found in T2* values among the different subgroups.

When adjusted with Holm-Bonferroni procedure none of the significant comparisons were significant.

4. Discussion

This study suggests a potential link between increasing brain iron load and both motor and cognitive performances in patients with PD. Previous studies have investigated brain iron load and its impact on motor performances, reporting a relationship between the 2 (Zhang et al., 2009, 2010).

In our study, we observed an inverse correlation between T2*-weighted image values of the SN and both disease duration and UPDRS-III off, whereas UPDRS-III on was not related to T2*-weighted image values of the SN. Therein, it is plausible that UPDRS off indicated the true state of the disease, in terms of severity.

A few studies have tried to correlate brain iron and cognitive features in patients with PD failing to show differences between patients with PD with or without cognitive dysfunction (Zhang et al., 2009). Our study, instead, examined patients at 2 levels of neuropsychological assessment, as recommended by the MDS Task Force, providing positive results (Litvan et al., 2012). Specifically, iron accumulation was significantly related to MoCA both in the SN and in the GP. Meanwhile, when using MMSE, the relationship was

significant only in the GP. This is likely because of the greater sensibility of MoCA in detecting early baseline and longitudinal cognitive impairment in patients with PD, when compared with MMSE (Hu et al., 2014).

The second level of cognitive evaluation revealed that both Graded Naming Test and Spatial Span results correlated with T2*-weighted image values of the SN. Moreover, *WAIS-R Similarities* results were related to all the considered ROIs. The fact that this test explores conceptualization and executive functions, cognitive domains early affected in patients with PD, might well explain the alteration of multiple brain areas (Muslimovic et al., 2005).

Although in the past different MRI techniques have been used to investigate brain iron pattern in PD, no clear clinical correlation was found. This failure was possibly because of technical reasons (Barbosa et al., 2015; Rossi et al., 2013; Wallis et al., 2008). This is the main reason why physicians are searching for new MR protocols and parameters to better quantify brain iron deposits. Particularly, quantitative susceptibility mapping can detect with great efficacy local magnetic changes that are sensitive to metals like iron (Guan et al., 2017b), as demonstrated also by the comparison with histologic findings (Mechelle et al., 2018). Previous studies reported that patients with PD can be distinguished from healthy subjects using susceptibility-weighted imaging and the most involved areas were CN, RN (Zhang et al., 2009), GP (Rossi et al., 2014; Wang et al., 2012), and SN (Reiter et al., 2015; Rossi et al., 2014; Zhang et al., 2010). Moreover, susceptibility-weighted imaging values of the SN have been reported to correlate with both disease duration and *UPDRS* score (Jin et al., 2011; Zhang et al., 2010). Furthermore, increased iron deposit has been detected in the anterior region of the GP in patients with greater postural instability (Rossi et al., 2014) and in the DN in patients with higher tremor severity (Guan et al., 2017a). Iron content of the SN has been associated with the *Montgomery Asberg Depression Rating Scale* and *Hamilton Anxiety Scale* scores (An et al., 2018).

We accept that the ROI method lacks spatial precision, is time-consuming, and is limited by its hypothesis-driven nature (Yu et al., 2017). Differently, the normalization procedure used in whole-brain studies tends to attenuate group differences that are forced into a common standard space. Moreover, whole-brain analysis, then the ROI approach, is not applicable when the investigation is direct to regional changes, such as our experimental design, considering that the 2 methods were comparable in other settings.

Our study has a few limitations. First of all, sample size was limited and unbalanced toward a greater proportion of patients compared with control subjects. We are currently in the process of collecting further similar samples and making these analyses in another more extensive cohort. Second, we used a manual-tracing method to draw the brain structures, leading to a limitation because of subjective evaluation and time-consuming problems. Third, several neuropathologic aspects, such as metal deposition and loss of dopaminergic cells, can modify SN structure inducing atrophy and signal changes. In PD, the MRI studies also showed that the SN presents different signal changes in different MRI contrasts or methods (Lehéricy et al., 2014). In particular, neuromelanin, that is mainly distributed in locus coeruleus and substantia nigra pars compacta and that is increased in neurodegeneration, has a T1-shortening effect when combined with metals and by magnetic intensity (the prolongation of the T1 relaxation time at 3 T is higher than 1.5 T). Single parameter is not sufficient to characterize SN, whereas the multimodal method through the combination of techniques, as R2* and fractional anisotropy, could provide additional and complementary information for characterizing SN quantification (Péran et al., 2010). Moreover, several studies pointed out that iron has a bimodal deposition increasing in substantia nigra pars compacta in early stage and in substantia nigra pars reticulata only in more advanced stage of the disease (Guan et al., 2017c).

5. Conclusion

The main finding of our study is that iron load of the SN correlates with the majority of motor and cognitive parameters. Noteworthy, although our results are in line with previous findings suggesting that increased iron load of the SN reflects motor disabilities, they also suggest that nigral iron deposition influences decline of cognitive abilities, in particular of executive functions.

Disclosure

The authors have no actual or potential conflicts of interest. This research did not receive any specific grant from funding agencies in the public, commercial, or not-for-profit sectors.

Acknowledgements

The Movement Disorders Center of the University of Perugia was supported by a grant from the New York University School of Medicine and the Marlene and Paolo Fresco Institute for Parkinson's and Movement Disorders, which was made possible with support from Marlene and Paolo Fresco.

References

Aarsland, D., Creese, B., Politis, M., Chaudhuri, K.R., Ffytche, D.H., Weintraub, D., Ballard, C., 2017. Cognitive decline in Parkinson disease. Nat. Rev. Neurol. 13, 217–231.

An, H., Zeng, X., Niu, T., Li, G., Yang, J., Zheng, L., Zhou, W., Liu, H., Zhang, M., Huang, D., Li, J., 2018. Quantifying iron deposition within the substantia nigra of Parkinson's disease by quantitative susceptibility mapping. J. Neurol. Sci. 386, 46–52.

Anderson, G.J., Frazer, D.M., McLaren, G.D., 2009. Iron absorption and metabolism. Curr. Opin. Gastroenterol. 25, 129–135.

Apostolakis, S., Kypraiou, A.M., 2017. Iron in neurodegenerative disorders: being in the wrong place at the wrong time? Rev. Neurosci. 28, 893–911.

Barbosa, J.H., Santos, A.C., Tumas, V., Liu, M., Zheng, W., Haacke, E.M., Salmon, C.E., 2015. Quantifying brain iron deposition in patients with Parkinson's disease using quantitative susceptibility mapping, R2 and R2*. Magn. Reson. Imaging 33, 559–565.

Bartzokis, G., Tishler, T.A., Shin, I.S., Lu, P.H., Cummings, J.L., 2004. Brain ferritin iron as a risk factor for age at onset in neurodegenerative diseases. Ann. N. Y. Acad. Sci. 1012, 224–236.

Brazzelli, M., Capitani, E., Della Sala, S., Spinnler, H., Zuffi, M., 1994. A neuropsychological instrument adding to the description of patients with suspected cortical dementia: the Milan Overall Dementia Assessment. J. Neurol. Neurosurg. Psychiatry 57, 1510–1517.

Brooks, D.J., Tambasco, N., 2016. Imaging synucleinopathies. Mov. Disord. 31, 814–829.

Caffarra, P., Gardini, S., Zonato, F., Concari, L., Dieci, F., Copelli, S., Freedman, M., Stracciari, A., Venneri, A., 2011. Italian norms for the Freedman version of the Clock drawing test. J. Clin. Exp. Neuropsychol. 33, 982–988.

Cambridge Cognition, 2006. CANTABeclipseTM Version 3: Software user guide. Ed. Cambridge Cognition Ltd, Cambridge, UK.

Carlesimo, G.A., Sabbadini, M., Fadda, L., Caltagirone, C., 1995. Different components in word-list forgetting of pure amnesics, degenerative demented and healthy subjects. Cortex 31, 735–745.

Carlesimo, G.A., Caltagirone, C., Gainotti, G.U.I.D., Fadda, L., Gallassi, R., Lorusso, S., Parnetti, L., 1996. The mental deterioration battery: normative data, diagnostic reliability and qualitative analyses of cognitive impairment. Eur. Neurol. 36, 378–384.

Cormack, F., Aarsland, D., Ballard, C., Tovée, M.J., 2004. Pentagon drawing and neuropsychological performance in dementia with Lewy bodies, Alzheimer's disease, Parkinson's disease and Parkinson's disease with dementia. Int. J. Geriatr. Psychiatry 19, 371–377.

Ding, B., Gentleman, R., 2005. Classification using generalized partial least squares. J. Comput. Graphical Stat. 14, 280–298.

Folstein, M.F., Folstein, S.E., McHugh, P.R., 1975. 'Mini-Mental State'. A practical method for grading the cognitive state of patients for the clinician. J. Psychiatr. Res. 12, 189–198.

Gill, D.J., Freshman, A., Blender, J.A., Ravina, B., 2008. The montreal cognitive assessment as a screening tool for cognitive impairment in Parkinson's disease. Mov. Disord. 23, 1043–1046.

Goetz, C.G., Poewe, W., Rascol, O., Sampaio, C., Stebbins, G.T., Counsell, C., Giladi, N., Holloway, R.G., Moore, C.G., Wenning, G.K., Yahr, M.D., Seidl, L., Movement Disorder Society Task Force on Rating Scales for Parkinson's Disease, 2004. Movement disorder society task force report on the Hoehn and Yahr staging scale: status and recommendations. Mov. Disord. 19, 1020–1028.

Goetz, C.G., Tilley, B.C., Shaftman, S.R., Stebbins, G.T., Fahn, S., Martinez-Martin, P., Poewe, W., Sampaio, C., Stern, M.B., Dodel, R., Dubois, B., Holloway, R., Jankovic, J., Kulisevsky, J., Lang, A.E., Lees, A., Leurgans, S., LeWitt, P.A., Nyenhuis, D., Olanow, C.W., Rascol, O., Schrag, A., Teresi, J.A., van Hilten, J.J., LaPelle, N., Movement Disorder Society UPDRS Revision Task Force, 2008. Movement disorder society-sponsored revision of the Unified Parkinson's disease rating scale (MDS-UPDRS): scale presentation and clinimetric testing results. Mov. Disord. 23, 2129–2170.

Guan, X., Xu, X., Zhang, M., 2017a. Region-specific iron measured by MRI as a biomarker for Parkinson's disease. Neurosci. Bull. 33, 561–567.

Guan, X., Xuan, M., Gu, Q., Xu, X., Huang, P., Wang, N., Shen, Z., Xu, J., Luo, W., Zhang, M., 2017b. Influence of regional iron on the motor impairments of Parkinson's disease: a quantitative susceptibility mapping study. J. Magn. Reson. Imaging 45, 1335–1342.

Guan, X., Xuan, M., Gu, Q., Huang, P., Liu, C., Wang, N., Xu, X., Luo, W., Zhang, M., 2017c. Regionally progressive accumulation of iron in Parkinson's disease as measured by quantitative susceptibility mapping. NMR Biomed. 30, e3489.

Haacke, E.M., Ayaz, M., Khan, A., Manova, E.S., Krishnamurthy, B., Gollapalli, L., Ciulla, C., Kim, I., Petersen, F., Kirsch, W., 2007. Establishing a baseline phase behavior in magnetic resonance imaging to determine normal vs. abnormal iron content in the brain. J. Magn. Reson. Imaging 26, 256–264.

Haacke, E.M., Mittal, S., Wu, Z., Neelavalli, J., Cheng, Y.-C.N., 2009. Susceptibility-weighted imaging: technical aspects and clinical applications, Part 1. Am. J. Neuroradiol. 30, 19–30.

Hallgren, B., Sourander, P., 1958. The effect of age on the non-haemin iron in the human brain. J. Neurochem. 3, 41–51.

Hu, M.T., Szewczyk-Królikowski, K., Tomlinson, P., Nithi, K., Rolinski, M., Murray, C., Talbot, K., Ebmeier, K.P., Mackay, C.E., Ben-Shlomo, Y., 2014. Predictors of cognitive impairment in an early stage Parkinson's disease cohort. Mov. Disord. 29, 351–359.

Jin, L., Wang, J., Zhao, L., Jin, H., Fei, G., Zhang, Y., Zeng, M., Zhong, C., 2011. Decreased serum ceruloplasmin levels characteristically aggravate nigral iron deposition in Parkinson's disease. Brain 134 (Pt 1), 50–58.

Katz, S., Ford, A.B., Moskowitz, R.W., Jackson, B.A., Jaffe, M.W., 1963. Studies of illness in the aged: the index of ADL: a standardized measure of biological and psychosocial function. JAMA 185, 914–919.

Ke, Y., Qian, Z.M., 2003. Iron misregulation in the brain: a primary cause of neurodegenerative disorders. Lancet Neurol. 2, 246–253.

Kuhn, M., 2008. Caret package. J. Stat. Softw. 28, 1–26.

Lawton, M.P., Brody, E.M., 1969. Assessment of older people: self-maintaining and instrumental activities of daily living. Gerontologist 9, 179–186.

Lehéricy, S., Bardinet, E., Poupon, C., Vidaihlet, M., Francois, C., 2014. 7 Tesla magnetic resonance imaging: a closer look at substantia nigra anatomy in Parkinson's disease. Mov. Disord. 29, 1574–1581.

Litvan, I., Goldman, J.G., Tröster, A.I., Schmand, B.A., Weintraub, D., Petersen, R.C., Mollenhauer, B., Adler, C.H., Marder, K., Williams-Gray, C.H., Aarsland, D., Kulisevsky, J., Rodriguez-Oroz, M.C., Burn, D.J., Barker, R.A., Emre, M., 2012. Diagnostic criteria for mild cognitive impairment in Parkinson's disease: movement disorder society task force guidelines. Mov. Disord. 27, 349–356.

Martin, W.R., Wieler, M., Gee, M., 2008. Midbrain iron content in early Parkinson disease: a potential biomarker of disease status. Neurology 15, 1411–1417.

Mechelle, M.L., Guangwei, D., Baccon, J., Snyder, A.M., Murie, B., Cooper, F., Stetter, C., Kong, L., Sica, K., Mailman, R.B., Connor, J.R., Huang, X., 2018. Susceptibility MRI captures nigral pathology in patients with Parkinsonian syndromes. Mov. Disord. 33, 1432–1439.

Mochizuki, H., Yasuda, T., 2012. Iron accumulation in Parkinson's disease. J. Neural Transm. (Vienna) 119, 1511–1514.

Monaco, M., Costa, A., Caltagirone, C., Carlesimo, G.A., 2013. Forward and backward span for verbal and visuo-spatial data: standardization and normative data from an Italian adult population. Neurol. Sci. 34, 749–754.

Muslimovic, D., Post, B., Speelman, J.D., Schmand Muslimovic, B., 2005. Cognitive profile of patients with newly diagnosed Parkinson disease. Neurology 65, 1239–1245.

Novelli, G., Papagno, C., Capitani, E., Laiacona, M., 1986. Tre test clinici di ricerca e produzione lessicale. Taratura su sogetti normali. Arch. Psicol. Neurol. Psichiatria 47, 477–506.

Ordidge, R.J., Gorell, J.M., Deniau, J.C., Knigt, R.A., Helpern, J.A., 1994. Assessment of relative brain iron concentrations using T2-weighted and T2*-weighted MRI at 3 Tesla. Magn. Reson. Med. 32, 335–341.

Penke, L., Valdés Hernandéz, M.C., Muñoz Maniega, S., Gow, A.J., Murray, C., Starr, J.M., Bastin, M.E., Deary, I.J., Wardlaw, J.M., 2012. Brain iron deposits are associated with general cognitive ability and cognitive aging. Neurobiol. Aging 33, 510–517.e2.

Péran, P., Cherubini, A., Assogna, F., Piras, F., Quattrocchi, C., Peppe, A., Celsis, P., Rascol, O., Démonet, J.F., Stefani, A., Pierantozzi, M., Pontieri, F.E., Caltagirone, C., Spalletta, G., Sabatini, U., 2010. Magnetic resonance imaging markers of Parkinson's disease nigrostriatal signature. Brain 133, 3423–3433.

Postuma, R.B., Berg, D., Stern, M., Poewe, W., Olanow, C.W., Oertel, W., Obeso, J., Marek, K., Litvan, I., Lang, A.E., Halliday, G., Goetz, C.G., Gasser, T., Dubois, B., Chan, P., Bloem, B.R., Adler, C.H., Deuschl, G., 2015. MDS clinical diagnostic criteria for Parkinson's disease. Mov. Disord. 30, 1591–1601.

Reiter, E., Muelle, C., Pinter, B., Krismer, F., Scherfler, C., Esterhammer, R., Kremser, C., Schocke, M., Wenning, G.K., Poewe, W., Seppi, K., 2015. Dorsolateral nigral hyperintensity on 3.0T susceptibility-weighted imaging in neurodegenerative Parkinsonism. Mov. Disord. 30, 1068–1076.

Rossi, M., Ruottinen, H., Soimakallio, S., Elovaara, I., Dastidar, P., 2013. Clinical MRI for iron detection in Parkinson's disease. Clin. Imaging 37, 631–636.

Rossi, M., Ruottinen, H., Saunamäki, T., Elovaara, I., Dastidar, P., 2014. Imaging brain iron and diffusion patterns. A follow-up study of Parkinson's disease in the initial stages. Acad. Radiol. 21, 64–71.

Simpson, I.A., Ponnuru, P., Klinger, M.E., Myers, R.L., Devraj, K., Coe, C.L., Lubach, G.R., Carruthers, A., Connor, J.R., 2015. A novel model for brain iron uptake: introducing the concept of regulation. J. Cereb. Blood Flow Metab. 35, 48–57.

Tambasco, N., Belcastro, V., Sarchielli, P., Floridi, P., Pierguidi, L., Menichetti, C., Castrioto, A., Chiarini, P., Parnetti, L., Eusebi, P., Calabresi, P., Rossi, A., 2011. A magnetization transfer study of mild and advanced Parkinson's disease. Eur. J. Neurol. 18, 471–477.

Valdés Hernández, M., Allerhand, M., Glatz, A., Clayson, L., Muñoz Maniega, S., Gow, A., Royle, N., Bastin, M., Starr, J., Deary, I., Wardlaw, J., 2016. Do white matter hyperintensities mediate the association between brain iron deposition and cognitive abilities in older people? Eur. J. Neurol. 23, 1202–1209.

Wallis, L.I., Paley, M.N.J., Graham, J.M., Grünewald, R.A., Wignall, E.L., Jy, H.M., Griffiths, P.D., 2008. MRI assessment of basal ganglia iron deposition in Parkinson's disease. J. Magn. Reson. Imaging 28, 1061–1067.

Wang, Y., Butros, S.R., Shuai, X., Dai, Y., Chen, C., Liu, M., Haacke, E.M., Hu, J., Xu, H., 2012. Different iron-deposition patterns of multiple system atrophy with predominant Parkinsonism and idiopathetic Parkinson diseases demonstrated by phase-corrected susceptibility-weighted imaging. AJNR Am. J. Neuroradiol. 33, 266–273.

Ward, R.J., Zucca, F.A., Duyn, J.H., Crichton, R.R., Zecca, L., 2014. The role of iron in brain ageing and neurodegenerative disorders. Lancet Neurol. 13, 1045–1060.

Wechsler, D., 1987. Manual for Wechsler Memory Scale—Revised. The Psychological Corporation, New York, NY.

Wechsler, D., 2008. Wechsler Adult Intelligence Scale—Fourth Edition (WAIS–IV). The Psychological Corporation, San Antonio, TX.

Yu, J., Lam, C.L.M., Lee, T.M.C., 2017. White matter microstructural abnormalities in amnestic mild cognitive impairment: a meta-analysis of whole-brain and ROI-based studies. Neurosci. Biobehav. Rev. 83, 405–416.

Zecca, L., Youdim, M.B., Riederer, P., Connor, J.R., Crichton, R.R., 2004. Iron, brain ageing and neurodegenerative disorders. Nat. Rev. Neurosci. 5, 863–873.

Zhang, W., Sun, S.G., Jiang, Y.H., Qiao, X., Sun, X., Wu, Y., 2009. Determination of brain iron content in patients with Parkinson's disease using magnetic susceptibility imaging. Neurosci. Bull. 25, 353–360.

Zhang, J., Zhang, Y., Wang, J., Cai, P., Luo, C., Qian, Z., Dai, Y., Feng, H., 2010. Characterizing iron deposition in Parkinson's disease using susceptibility-weighted imaging: an in vivo MR study. Brain Res. 1330, 124–130.